*Chinese Journal of*
**POLYMER SCIENCE**

RESEARCH ARTICLE

https://doi.org/10.1007/s10118-022-2770-9
*Chinese J. Polym. Sci.* **2022**, *40*, 1050–1061

# Antibacterial Sutures Coated with Smooth Chitosan Layer by Gradient Deposition

Ying-Ge Chen, Chu-Xin Li, Yu Zhang, Yong-Dan Qi, Jun Feng*, and Xian-Zheng Zhang*

*Key Laboratory of Biomedical Polymers of Ministry of Education & Department of Chemistry, Wuhan University, Wuhan 430072, China*

Electronic Supplementary Information

**Abstract** Owing to the significant importance in clinics, antibacterial activity is thought as one indispensable feature of the next generation of absorbable sutures. It is challenging but imperative to arm the existing absorbable sutures with antibacterial functions. The present study describes a "gradient deposition" technique to coat a continuous and smooth layer of chitosan on the surface of absorbable sutures. Specifically, chitosan solution is arranged to undergo gradient pH decline step by step while during each pH interval, the solution is allowed to stand for a predetermined period of time in order to control gradual chitosan deposition. Chitosan nanoparticles are found to be first generated on suture surface and finally developed into a smooth chitosan layer as the antibacterial surface. *In vitro* and *in vivo* results demonstrated that coating chitosan on sutures by our technique could relieve wound inflammation, stimulate collagen deposition, regenerate blood vessels, and assist tissue repairing, consequently leading to a significant enhancement of wound healing effect. This technique is highlighted with low cost, extreme convenience and excellent safety without organic solvents. Furthermore, the "gradient deposition" technique would not affect the fundamental properties of matrix and thus hold promises as a universal way for superficial antibacterial modification towards almost all the surgical implanted materials, including but not limited to absorbable sutures.

**Keywords** Antibacterial sutures; Gradient deposition; Chitosan coating; Wound healing; Bacterial infection

**Citation:** Chen, Y. G.; Li, C. X.; Zhang, Y.; Qi, Y. D.; Feng, J.; Zhang, X. Z. Antibacterial sutures coated with smooth chitosan layer by gradient deposition. *Chinese J. Polym. Sci.* **2022**, *40*, 1050–1061.

## INTRODUCTION

Absorbable materials, particularly absorbable sutures with a global market value of $5.84 billion by 2023, are currently playing essential roles in surgical fields.[1,2] Absorbable sutures are all fabricated from biocompatible polymers that can degrade *in vivo* into nontoxic substances. Both the polymers and their degraded substances are required to have no antigenicity and minimal tissue reactions.[3] After implanted into body, absorbable sutures ought to maintain sufficient mechanical strength and structural integrity for a determined period of time to match well wound healing progress. In addition, absorbable sutures must possess high stability under harsh sterilization conditions.[4,5] Due to these strict demands, commercialized synthetic polymers have taken a leading position in market and they are mostly limited to aliphatic polyesters, such as polylactide (PLA) and poly(lactide-*co*-glycolide) (PLGA).[3]

Postoperative wounds are very susceptible to bacterial infection, which reaches as high as 12.5% in patients and exerts an adverse impact on wound healing.[6,7] Surgical site infections (SSIs) would lead to operation failure in some cases and are implicated in many complications and even the life-threatening risk. Of note, surgically implanted materials have been identified as one of the major contributory factors in SSIs,[8] particularly skin sutures with a long-term exposure to nonsterile environments. SSIs are commonly initiated by the bacterial attachment onto the surface of implanted materials to form a self-protection biofilm, allowing the colonization and migration of bacteria to infect surrounding tissues.[9] Oral administration of antibiotic drugs is clinically recommended at present to prevent bacterial infection. However, since this medication is a modality of systematic administration, high dosage is needed to ensure sufficient antibacterial activity in wound sites, inevitably causing side effects and inducing bacterial resistance.[1,10] Owing to the significant importance in clinics, antibacterial capability has been acknowledged as one indispensable feature of the next generation of sutures.

Antibacterial activity of sutures has to last for a long period prior to complete wound healing. A solution is to physically bury antibacterial drugs inside suture matrix. Although this approach permits the sustained antibacterial effect, it is bound to affect polymeric crystallization, matrix cohesion and cause structural heterogeneity inside suture matrix,[11,12] lead-

* Corresponding authors, E-mail: fengjun@whu.edu.cn (J.F.)
E-mail: xz-zhang@whu.edu.cn (X.Z.Z.)

Special Issue: Biomedical Polymers
Received March 30, 2022; Accepted May 9, 2022; Published online July 12, 2022

ing to serious destruction of suture-associated properties, such as considerable loss of mechanical strength, premature degradation and so on.[13] Designing new antibacterial suture materials might be an alternative option by chemical incorporating antibacterial agents into suture matrix or onto suture surface.[14,15] However, this approach needs complex chemistry that is involved in both material preparation and drug release. In addition, apart from antibacterial potency, these new sutures may not be suited for suture purpose in terms of other fundamental requirements, such as mechanical strength, degradation speed and safety.[12] Another concern for chemical introduction of antibacterial components arises from the commonly used melting-processing procedure for suture manufacture, in which high temperature is needed but it would more or less deactivate the introduced drugs.[9] Anyway, this approach represents a long and costly way toward clinical applications and appears to be not a preferred choice. Ideally, if antibacterial drugs can be physically attached onto suture surface, those mentioned issues would be overcome and meanwhile, the drugs on surface can take effect directly to inhibit the superficial formation of bacterial "biofilm". However, small-molecular antibacterial drugs fail to closely attach on the material surface. Moreover, since the adhered drugs is prone to free diffusion in aqueous solutions, sutures would experience unwanted burst release in the early stage once the contact with body fluids, resulting in a transient antibacterial activity with poor outcomes.[16–18]

As stated above, it is significantly challenging but imperative to arm the existing absorbable sutures with the antibacterial function. Chitosan, a derivative of chitin, is insoluble in most organic solvents and water solution with neutral and alkaline pHs, but soluble in acidic solutions.[19] Chitosan has excellent biodegradability and low toxicity to mammalian cells. As an outstanding advantage, chitosan possesses a wide range of antimicrobial activities against many drug-resistant microorganisms and does not produce bacterial resistance.[20] When the average molecular weight of chitosan is above 100 kDa, chitosan realizes antibacterial purpose mainly as physical barrier; antibacterial effect of chitosan below 10 kDa is provided by interfering with cell metabolic activities *via* electrostatic interactions.[21,22] Besides, chitosan containing abundant amino groups can relieve aseptic inflammation, which frequently occurs *in vivo* for polyester-based implanted materials, by neutralizing the degradation-caused acid condition.[23] Chitosan has been intensively studied for antibacterial applications. The major methods to fabricate chitosan-based coating include: (1) chemical bonding onto matrix; (2) electrostatically driven deposition by reacting chitosan with negatively charged polymers (*i.e.*, sodium alginate, hyaluronic acid); (3) integrating chitosan into other coating materials.[23,24] These methods are unfortunately not suitable for the currently existing sutures. For instance, the method of electrostatically driven deposition would neutralize the charge of chitosan and largely reduce its pharmacological effect.[25] The mixing method is restricted by the compatibility between different coating materials and the insufficient chitosan content.[9,26,27] From the perspective of practical translation, it is very meaningful to create a simple and cost-effective method that can attach a dense coating merely composed of chitosan on suture surface to acquire powerful antibacterial activity.

To address this challenge, the present study reported a "gradient deposition" technique to coat a continuous and smooth layer of chitosan on the surface of absorbable sutures. Specifically, chitosan solution was arranged to undergo gradient pH decline step by step. During each pH interval, the solution was allowed to stand for a predetermined period of time to control gradual chitosan deposition. Chitosan nanoparticles were found to be first generated on suture surface, the chitosan deposition gradually grew up and finally developed into a smooth chitosan layer as the antibacterial surface (Scheme 1). Interestingly, this method was found to be suitable to the commercialized absorbable sutures derived from synthetic and natural polymers in a matrix-independent manner. The continuous and smooth chitosan coating is bound to improve antibacterial performance and lower physical damages to tissues. In contrast, the conventional method by directly adjusting CS solution to predetermined pH without gradient deposition treatment failed to provide desired coating. This approach is also highlighted with low cost, extreme convenience and excellent biosafety without using organic solvents. Furthermore, the gradient deposition technique would not affect the fundamental properties of the coated matrix and thus hold promises as a universal way for superficial antibacterial modification toward almost all the surgical implanted materials, including but not limited to absorbable sutures.

## MATERIALS AND METHOD

### Materials

Chitosan (CS, MW=30k) with a degree of deacetylation at 0.85 was purchased from Macklin Biochemical Co., Ltd. Poly(lactic-*co*-glycolic acid) (PLGA-COOH) (MW=50k) was purchased from Xi'an ruixi Biological Technology Co., Ltd. Dichloromethane ($CH_2Cl_2$), acetic acid (HAC) and dimethylsulfoxide (DMSO) were purchased from Shanghai Reagent Chemical Co. (China). PGLA sutures were obtained from Shanghai Pudong Jinhuan Medical Products Co., Ltd. Catgut sutures were purchased from Shandong Boda Mecical Products Co., Ltd. DiR. Potassium hydroxide (KOH) was purchased from Sinopharm Chemical Reagent Co., Ltd. Agar and Luria-Bertani (LB) broth and agar were purchased from HuanKai Microbial Co., Ltd. (China). Ampicillin (98%) was purchased from Macklin Biochemical Co., Ltd. Propidium iodide (PI) was obtained from Sigma-Aldrich. MycoLight Green JJ98 was purchased from AAT Bioquest, Inc. Phosphate-buffered saline (PBS), Dulbecco's Modified Eagle's Medium (DMEM) and penicillin-streptomycin were purchased from Gibco Invitrogen Corp. Fetal bovine serum (FBS) was purchased from Biological Industries. 3-[4,5-Dimethylthiazol-2-yl]-2,5-diphenyltetrazolium-bromide (MTT) was supplied by Beyotime Biotechnology Co., Ltd. (China). General tissue fixative (4% paraformaldehyde) was obtained from Wuhan Servicebio Technology Co., Ltd. Enzyme linked immunosorbent assay (ELISA) kit for Recombinant murine IL-6 and TNF-$\alpha$ was purchased from 4A Biotech Co., Ltd. (Beijing, China), recombinant murine IL-10 kit was purchased from Shanghai Zeye Biotechnology Co., Ltd.

### Bacterial Strains

*Escherichia coli* ER2738 strain (*E. coli* ER2738) and *Escherichia coli*

https://doi.org/10.1007/s10118-022-2770-9

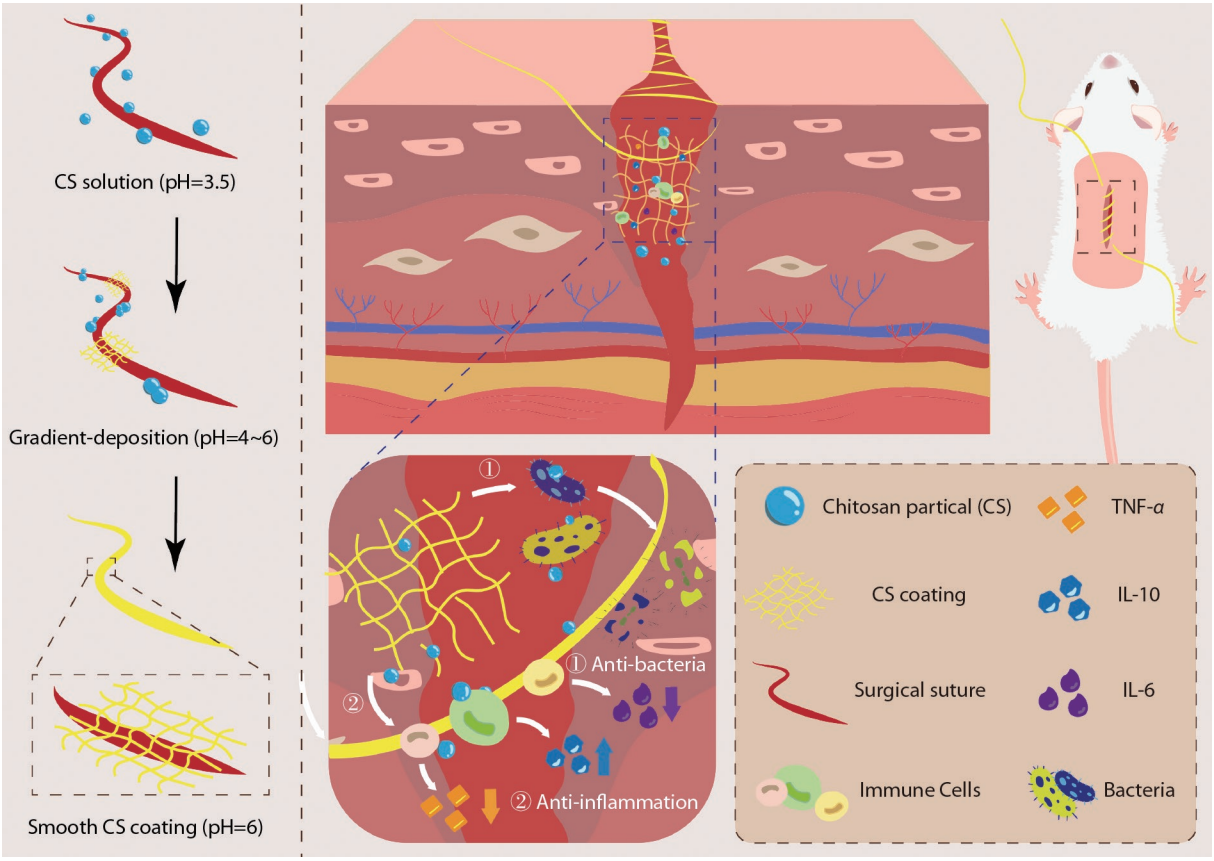


**Scheme 1** Synthesis process and illustration of multifunctional anti-inflammation and antibacterial properties of CS-coated suture for improved wound healing.

ATCC 25922 strain (*E. coli* 25922) were collected from the American Type Culture Collection (ATCC). *E. coli* mBL21 was achieved by introducing two plasmids into *E. coli* ER2738, which confers *E. coli* mBL21 with ampicillin resistance and mCherry protein expression.

## Cell Line and Cultured Conditions

3T3 murine embryonic fibroblast cells were obtained from the China Centre for Type Culture Collection (CCTCC) and cultured in DMEM, containing 10% FBS, 100 U/mL of penicillin-streptomycin, and incubated at 37 ℃ with 5% $CO_2$.

## Characterization Methods

Scanning electron microscope (SEM) images were obtained by Zeiss SIGMA scanning electron microscope (Carl Zeiss, UK). The fluorescence and bright imaging were performed with a living image IVIS® spectrum (Perkin-Elmer), inverted fluorescence microscope (IX53, Olympus), and upright fluorescence microscope (BX53, Olympus). The germination and growth of the bacteria was measured by a Microplate reader (Bio-Rad, Model 550).

## Preparation of CS-coated Membrane and CS-coated Sutures

CS (11.25 g) was added in 250 mL of deionized water with stirring, and dissolved in pH 3.5 by HAC (4.5% CS solution). For CS-coated membrane, PLGA (90 mg) was dissolved in 15 mL of dichloromethane ($CH_2Cl_2$) by stirring. Then, 1.5 mL of solution was added into 35 mm glass culture dish and placed 2 h for solvent evaporation, and then dried in vacuum. In this way, PLGA was obtain as membrane. Next, 3 mL of 4.5% CS solution was incubated with PLGA membrane. Using 0.08 mol/L KOH solution, the pH of CS solution was adjusted to 4.0 and stand for 30 min, then adjusted to 5.0 and stand for 30 min, and at last adjusted to 6.0 to stand for 6 h. After, the upper layer liquid was removed, the membrane was washed with deionized water for three times, and then dried in vacuum to produce CS-coated membrane (Membrane@CS). CS-coated sutures were prepared in a similar way. In brief, 90 mm of PGLA/Catgut sutures were immersed in 8 mL of 4.5% CS solution. Using 0.1 mol/L KOH solution, the pH of CS solution was adjusted to 4.0 and stand for 30 min, then adjusted to 5.0 and stand for 30 min, at last adjusted to 6.0 to stand for 12 h. After, the upper layer liquid was removed, the sutures were washed with deionized water for three times, and then dried in vacuum to produce CS-coated sutures (sPGLA@CS, sCatgut@CS).

## *In vitro* Anti-bacterial Assay of Membrane@CS

LB broth (3 mL, with 100 μg/mL ampicillin) was added into glass culture dish with Membrane@CS and controls, then *E. coli* mBL21 during logarithmic phase growth ($10^7$ CFU/mL, 3 μL) was added to the medium (3 mL) and cultured with Membrane@CS for 12 h at 37 ℃. Thereafter, 100 μL of co-cultured bacteria was collected in 96-well dish, the germination and growth of the bacteria was measured by Microplate reader at 600 nm (OD600).

https://doi.org/10.1007/s10118-022-2770-9

Then, the rest co-cultured bacteria were diluted and cultured in LB agar (with 100 μg/mL ampicillin) for 12 h at 37 °C. The bacteria were evaluated as log reduction of the colony forming units (CFU/mL). The mCherry protein fluorescence imaging of *E. coli* mBL21 on LB agar was performed with a living image IVIS® spectrum.

### Oscillation Flask Method for sPGLA@CS/sCatgut@CS Antibacterial Assay

3 cm of sPGLA@CS, sCatgut@CS and controls were immersed into 1 mL of LB broth (with 100 μg/mL ampicillin) which inoculated with *E. coli* mBL21 ($10^7$ CFU/mL, 100 μL), and incubated at 37 °C for 1 h in the normoxia laboratory shaker (180 r/min). Then, serial dilutions of cultured-bacteria were made and spread onto LB agar and incubated overnight at 37 °C. The initial number of *E. coli* mBL21 before incubated with sutures were also been tested. The adherent viable bacteria to the sutures were evaluated as log reduction of the colony forming units (CFU/mL). The mCherry protein fluorescence imaging of *E. coli* mBL21 on LB agar was performed with a living image IVIS® spectrum. The antibacterial efficiency is evaluated as following rule ($n$=3):

$$\text{Antibacterial activity (\%)} = \frac{\text{CFU}_{(\text{Before})} - \text{CFU}_{(\text{Samples})}}{\text{CFU}_{(\text{Before})}} \times 100\% \quad (1)$$

where $\text{CFU}_{(\text{Before})}$ means the initial bacteria number before incubated with sutures.

### Anti-biofilm Assay of sPGLA@CS and sCatgut@CS

3 cm of CS-coated sutures and controls were immersed into 1 mL of LB broth (with 100 μg/mL ampicillin) which inoculated with *E. coli* mBL21 ($10^7$ CFU/mL, 100 μL), and incubated at 37 °C for 2 h. Then, incubated sutures were stained by MycoLight Green JJ98 ($1\times10^{-6}$ mol/L) and PI solutions ($4\times10^{-4}$ mol/L) for 20 min away from light. Live bacteria (stained green) and dead bacteria (stained red) are visualized on sutures using an inverted fluorescence microscope.

### *In vitro* Cytocompatibility Analysis

The cytocompatibility analysis of CS coating sutures was evaluated by MTT assays. 3 cm of CS-coated sutures and the control groups sutures were respectively incubated with 2.5 mL of DMEM medium in 24-well plates overnight, and 3T3 cells were seeded in 96-well plates ($1\times10^4$ per well) and cultured for 12 h in DMEM medium. Then, the cell supernatant was replaced with different concentrations (25%, 50%, 75%, 100%) of suture-incubated medium and continued co-cultured for another 24 h. After that, 20 μL of MTT (5 mg/mL) was added and incubated for 4 h, and the medium with MTT was removed and supply with 150 μL of DMSO solution. Absorbance at 570 nm was measured Microplate reader (Molecular devices). The cell viability is counted as follows ($n$=6):

$$\text{Cell viability} = \frac{\text{OD}_{(\text{sample})}}{\text{OD}_{(\text{BLANK})}} \times 100\% \quad (2)$$

where $\text{OD}_{(\text{BLANK})}$ means the absorbance of untreated 3T3 cells in MTT assay at 570 nm. The samples are referred to as sPGLA, sCatgut, sPGLA+CS, sCatgut+CS, sPGLA@CS and sCatgut@CS.

### *In vivo* Wound-Healing and Anti-Inflammation Examinations

The *in vivo* wound healing experiments were conducted on the linear excisional wound model in 8–10 weeks Balb/C female mice. Before experiment, the dorsal hairs of mice were removed and a 20 mm full-thickness incision was cutting on the center area of back in each mouse. Then, three mice were randomly divided into each group, including untreated wound and wound closed by sPGLA, sCatgut, sPGLA+CS, sCatgut+CS, sPGLA@CS and sCatgut@CS. The photos of wounds were taken every two days (1, 3, 5, 7 day). Wound tissues were harvested form each group mice for wound microenvironment analyzed. The wound tissues were fixed with 4% paraformaldehyde for hematoxylin and eosin (H&E) and Masson's trichrome stain. Wound tissues surrounding cytokines (IL-6, IL-10, TNF-$\alpha$) were detected by ELISA kit assay. And IL-6, TNF-$\alpha$ and CD31 immunofluorescence staining were employed for the detection of inflammatory and angiogenic responses at wound sites. Here, H&E staining, Masson's staining, and IL-6, IL-10, TNF-$\alpha$ ELISA assay and immunohistochemical staining were employed on day 4. CD31 immunofluorescence staining were employed on day 7. H&E, Masson's trichrome sections and immunofluorescence sections were observed with an upright fluorescence microscope and an inverted fluorescence microscope, respectively.

### *In vivo* Pathogen Acute Infection Wound Model

The excisional wound model was established as described above. Then, 50 μL of *E. coli* 25922 ($1\times10^8$ CFU/mL) was introduced into the wound in drop-by-drop fashion. The pictures of wound sites were taken after 0, 1, 2, 3, 5, 7, 9 and 14 days. The wound infection areas were calculated by Image J.

## RESULTS AND DISCUSSION

### Preparation and Characterization of CS-coated PLGA Membranes by "Gradient Deposition" Technique

In order to provide a universally applicable coating method to endow sutures with an antibacterial activity, we intended to fabricated a CS coating layer on sutures in a simple pathway. By adjusting CS solution to a higher pH, CS is bound to separate from aqueous solution owing to the pH-dependent protonation/deprotonation of amino groups contained in CS. However, the formation of continuous CS coating is challenged by the difficult control over deposition. In other words, it is uncertain whether the CS isolated from aqueous solution could finally form an evenly distributed coating with ordered structure on suture surface. The result verified our anxiety that there appeared a large amount of precipitate in solution and the precipitated CS failed to closely attach to sutures. Alternatively, we attempted to split the pH adjusting process into several pH intervals. For example, CS solution at pH 4.0 was first adjusted to pH 5.0 followed by the standing for 30 min. This neutralization-standing process was repeated again to the end at pH 6.0. Finally, the solution continued to stand for a couple of hours. The incubated absorbable materials were then taken out and washed with pure water thrice. We termed this treatment as the "gradient deposition" technique and conjectured it may bring about good outcomes beyond expectation.

To optimize "gradient deposition", the factors including the initial concentration of CS solution, standing time post pH adjusting were studied. To simplify *in vitro* studies, a PLGA mem-

https://doi.org/10.1007/s10118-022-2770-9

brane instead suture was immersed in 3% CS solution with pH 3.5, the co-cultured solution was subjected to "gradient deposition" using 0.1 mol/L KOH solution as the pH regulator. The pH of three CS solutions was respectively adjusted to three values (4.0, 5.0 and 6.0) in 1.5 h by three pH intervals. Thereafter, solution continued to be incubated with membrane for several hours for better film formation. As shown in Fig. 1(a), adjusting solution to pH 6 as the terminal point leads to better antibacterial outcomes. This result is understandable in view of the chitosan p$K_a$ at 6.3. Too low ending pH means less isolation of CS from aqueous solution. When the ending pH was fixed at 6, the influences of the initial concentration of CS solutions, the standing time post pH adjusting were examined (Figs. 1b and 1c). Apparently, longer standing time and the higher initial concentration contributed more or less to the improved antibacterial performances. In addition, it appeared that pure water was superior over ethanol for coating washing in terms of the antibacterial efficiency. Eventually, the optimal conditions were chosen as following: 4.5% CS solution was successively adjusted to 6.0 with three pH intervals (4.0, 5.0 and 6.0) and 30 min in each interval. The solution was then allowed to stand for 6 h and was finally washed by pure water thrice.

The obtained CS-coated PLGA Membrane (Membrane@CS) could defense almost 99% of *E. coli* mBL21 bacteria (an ampicillin-resistant *Escherichia coli* expressing mCherry fluorescence protein) compare to the bare PLGA membrane (Fig. 1d). To make clear whether the "gradient deposition" technique could endow PLGA membrane with a long-term antibacterial coating, Membrane@CS were immersed for 1, 3, 5, 7 days, respectively, in PBS buffer solution to mimic the *in vivo* condition (Fig. 1d). Results show that even after 7 days of incubation, Membrane@CS still retains good antibacterial activities (83.3% against *E. coli* mBL21). This result indicated that by means of this technique, the formed CS coating can closely attach on PLGA membrane with high stability.

To confirm that CS layer was actually coated on Membrane@CS surface, the elemental mapping by a high-angle annular dark field scanning transmission electron microscopy (HAADF-STEM) was conducted. Results manifest the even distribution of N element belonging to CS on the Mermbrane@CS surface (Fig. 1e). The CS solution was directly adjusted to pH 6.0 without gradient deposition treatment followed by the standing for 7.5 h. The obtained membrane (Membrane+CS) was taken as the control to validate the superiority of gradient deposition. The *in vitro* antibacterial activity against *E. coli* mBL21 was next compared among Membrane, Membrane+CS and Membrane@CS (Fig. 1f). The results show that the obtained Membrane@CS possesses a much stronger antibacterial activity compared to the other group. All these encouraging results stimulated us to explore the anti-bacterial performance of CS-coated sutures both *in vitro* and *in vivo*.

To probe the mechanism of CS coating by gradient deposition, the morphology of Membrane@CS samples prepared with different standing time were observed by SEM (Fig. S1 in the electronic supplementary information, ESI). Uncoated PLGA membrane displays a clean and smooth surface. Membrane@CS exhibits the extremely smooth and mirror-like surface. In the initial stage of the whole "gradient deposition" process, there occurred particles attachment before the formation of smooth coating layer. According to the finally formed smooth surface, it is speculated that CS layer were possibly generated through slow growth surrounding these particles. More detailed studies are needed to make clear the exact mechanism.

## Preparation and *In vitro* Antibacterial Characterization of CS-coated Sutures

Surgical sutures play clinically essential roles in facilitating incision closure. However, there are more opportunities for exotic intruders to induce and exacerbate bacterial infection. Therefore, wound sutures with antibacterial capability are of great importance in surgery fields. Here, the antibacterial efficacy of CS-coated sutures against *E. coli* mBL21 was fully assessed. Two widely used commercialized sutures, braided PGLA polymer suture (sPGLA) and Catgut suture (sCatgut), were selected as typical models to prepare CS-coated sutures, which were named as sPGLA@CS and sCatgut@CS, respectively. Similar to that of PLGA membrane, the controls named sPGLA+CS and sCatgut+CS were prepared for comparison. The PGLA sutures were observed by SEM. sPGLA@CS shows a very smooth surface and the gaps among the threads of sutures are filled with CS (Fig. 2a). In comparison, sPGLA+CS with rough surface still reserves the gap among polymer fibers, suggesting the difficult attachment of the rapidly precipitated CS particles. These results reconfirmed the strong affinity of CS coating on PGLA materials regardless of their shapes, such as membrane and thread. The evaluation over antibacterial activities of sutures was conducted by the oscillation flask method. 3 cm of sPGLA, sCatgut, sPGLA+CS, sCatgut+CS, sPGLA@CS, and sCatgut@CS were immersed into 1mL of bacterial medium and incubated for 1 h, respectively. As shown in Figs. 2(b) and 3(c) and Tables S1 and S2 (in ESI), sPGLA+CS and sCatgut+CS exhibit the similarly poor antibacterial activity. In comparison, both sPGLA@CS, and sCatgut@CS demonstrate excellent inhibition against *E. coli* mBL21 growth.

Biofilm formation is known as the "public enemies" in chronic/acute infection. Biofilm represents a protection mode in micro-organisms growth and allows them to survive in hostile environments and migrate to generate new colonies in other areas of the host.[28–30] Implanted sutures could serve as the refuge harbor for long-term bacterial colonization.[31,32] The post-surgery wound is vulnerable to bacterial infection and the improper medical practices would augment this risk.[33–35] Thus, the anti-biofilm efficiency of surgical sutures is an important index reflecting the antibacterial activity. Hence, we investigated the biofilm adhesion and formation of *E. coli* mBL21 on sutures by Live/Dead bacteria staining method, in which dead bacteria were stained red by nuclei staining dye propidium iodide (PI), and live bacteria were stained green by MycoLight Green JJ98 (Fig. 2d). In groups of sPGLA, sCatgut, sPGLA+CS, sCatgut+CS, green fluorescence fully cover suture surface with high intensity, clearly indicating the contiguous biofilm formation and adhesion on sutures. In contrast, green fluorescence is almost undetectable in groups of sPGLA@CS and sCatgut@CS while red fluorescence appeared with strong intensity instead, suggesting the strong

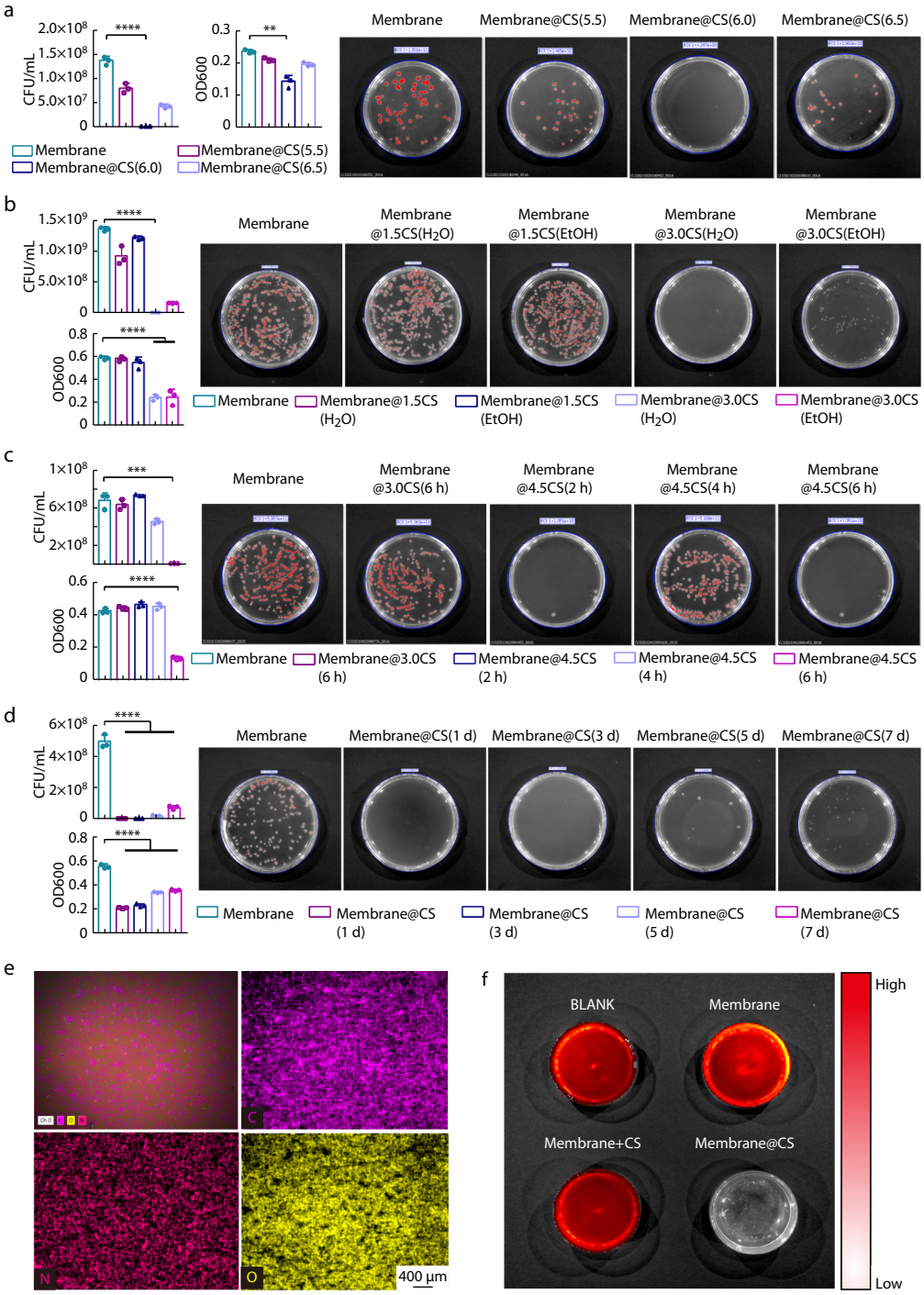


**Fig. 1** Characterization of CS-coated PLGA membrane. (a) Optimization results of CS pH including: the number of co-cultured *E. coli* mBL21 colony-forming units on LB agar plate, the mean absorbance value (optical density, OD) of co-cultured *E. coli* mBL21 liquid at 600 nm, and the representative fluorescence images of bacteria co-cultured with different membranes. "Membrane@CS (5.5)" means CS solution was eventually adjusted to pH 5.5, other groups follow this naming rule. (b) Optimization results of initial CS concentration and materials post-treatment methods, "Membrane@3%CS($H_2O$)" means the CS-coated membrane was prepared in 3% CS solution and finally washed by $H_2O$. Other groups follow this naming rule. (c) Optimization results of standing time after pH adjusting. "Membrane@4.5%CS(6h)" means that 4.5% CS solution was allowed to stand for 6 h after pH adjusting. Other groups follow this naming rule. (d) Variation of *in vitro* antibacterial activity of CS-coated membrane as incubation time. Membrane@CS was immersed in PBS buffer for 1, 3, 5, 7 days, respectively. (e) Element mapping of Membrane@CS. Scale bar=400 μm. (f) Representative fluorescence images of bacteria co-cultured with different membranes. The fluorescence intensity in plates images represented the mCherry protein activity in cultured *E. coli* mBL21. All data were shown as mean with SD. Statistical significance was calculated by one-way ANOVA. ***$p$<0.001, ****$p$<0.0001.

https://doi.org/10.1007/s10118-022-2770-9

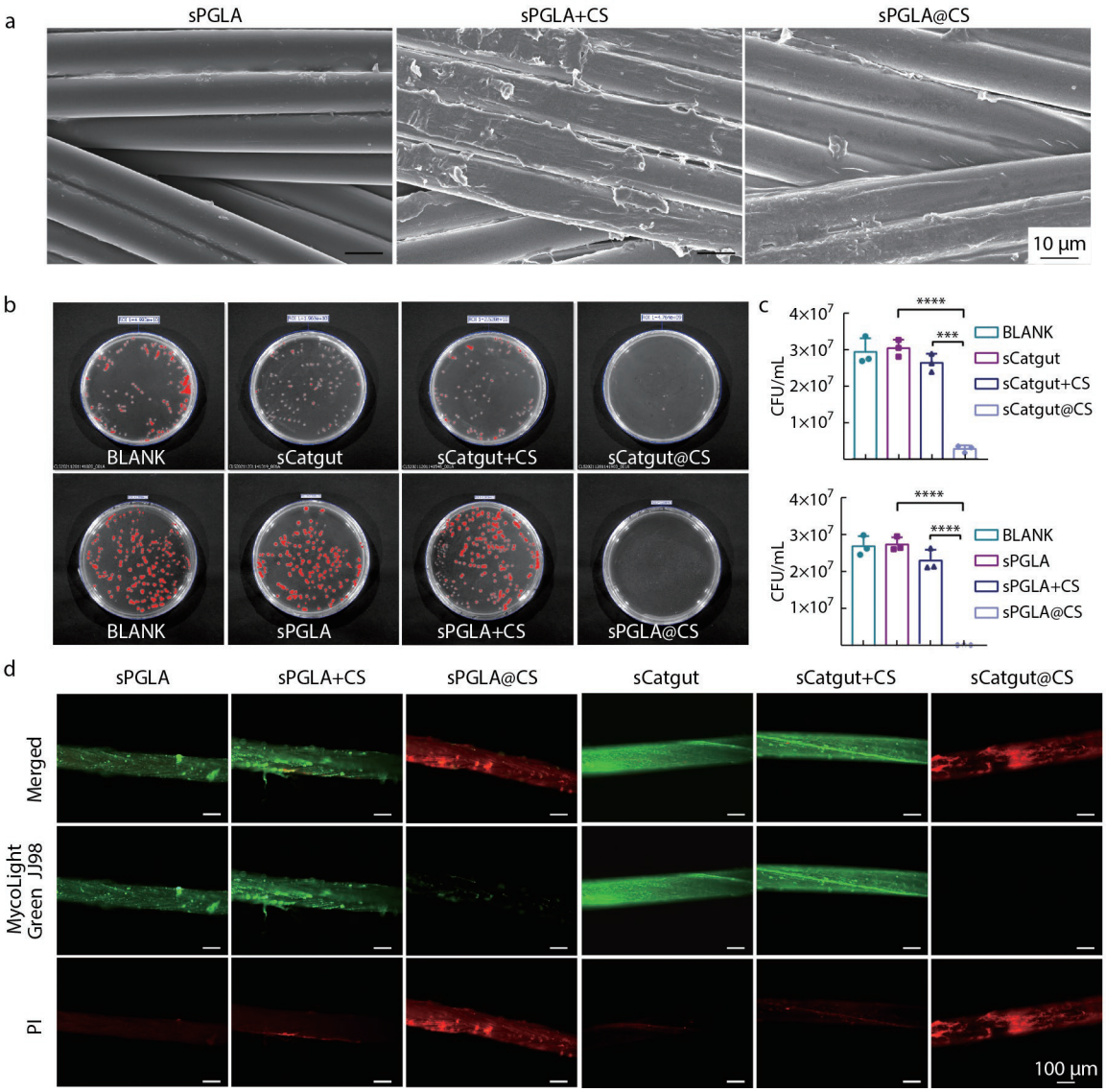


**Fig. 2** *In vitro* anti-bacterial and anti-biofilm performances. (a) SEM images of sPGLA, sPGLA+CS, sPGLA@CS. Scale bar=10 μm. (b, c) Antibacterial results sPGLA, sCatgut, sPGLA+CS, sCatgut+CS, sPGLA@CS, and sCatgut@CS by oscillation flask method. (d) Fluorescence images of sPGLA, sCatgut, sPGLA+CS, sCatgut+CS, sPGLA@CS, and sCatgut@CS after the incubation with *E. coli* mBL21. Live bacteria were stained green using MycoLight Green JJ98 and dead bacteria were stained red using PI. Scar bar=100 μm. All data are shown as mean with SD. Statistical significance was calculated by one-way ANOVA. ***$p$<0.001, ****$p$<0.0001.

anti-biofilm activities against *E. coli* mBL21.

### *In vivo* Biocompatibility and Influences of CS-coated Sutures on Wound Healing and Tissue Regeneration

CS-coated sutures were demonstrated with good anti-bacterial and anti-biofilm activities *in vitro*. Before the *in vivo* antibacterial evaluation, regular wound healing assay of CS-coated sutures were carried out in the normal wound model. Since sPGLA and sCatgut are widely used medical biomaterials with no toxicity,[36] they were used as the controls for biosafety evaluation in cellular levels by MTT assay (Fig. 3a). According to the established method,[37,38] all sutures were immersed in fresh cell culture medium overnight, the incubating solution was isolated and diluted into five concentrations (0%, 25%, 50%, 75%, 100%) to co-culture normal 3T3 cell (murine embryonic fibroblast) for 12 h. MTT results show no significant differences in cell proliferation between all groups ($p$>0.1), indicating that CS coating exerted minimal influences over the biocompatibility of raw sutures. This result is rational when the contact attachment of CS coating and the high biocompatibility of CS are considered.

Next, we assessed the contribution of CS-coated sutures to the healing of the *in vivo* established wounds by using sPGLA@CS as the typical model. 20 mm Incision was made on the back center of 8–10 weeks Balb/C female mice. Mice with untreated wound were taken as the negative controls. Three mice were randomly allocated into each group ready for the treatments with different sutures, including sPGLA, sPGLA+CS, and sPGLA@CS. As shown in the images of wounds after operation, PGLA@CS-treated wounds present

https://doi.org/10.1007/s10118-022-2770-9

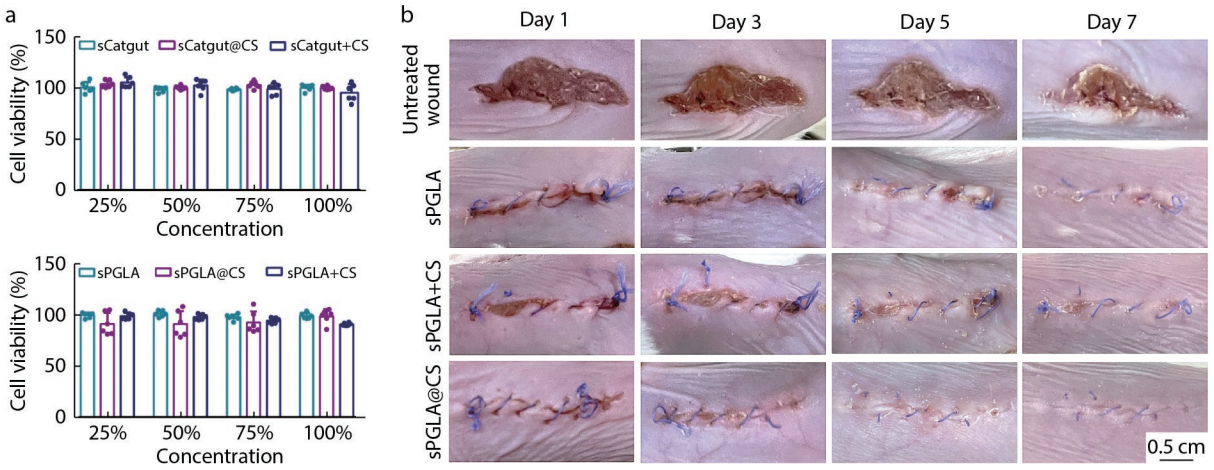


**Fig. 3** Biocompatibility assay and *in vivo* wound healing. (a) Cytocompatibility evaluation by MTT assays, suture-incubated cell mediums were diluted to different concentration (0%, 25%, 50%, 75%, 100%) to culture 3T3 cells for 12 h. (b) Representative images of wound treated with PGLA, PGLA+CS, PGLA@CS for 1, 3, 5 and 7 days. Scar bar=0.5 cm.

apparently better detumescence effect than other groups (Fig. 3b). On day 5 post suturing, sPGLA@CS group has almost completed the incision closure whereas that is barely achieved on day 7 in groups of sPGLA and sPGLA+CS. The similar result was obtained in the case of sCatgut@CS (Fig. S3 in ESI). Foreign intruders may induce abnormal wound healing accompanied by the formation of hypertrophic scars and keloids.[39] Apart from aesthetics concern, scarring-related tissue dysfunction remains a major healthcare challenge with limited treatment options. Thus, scar prevention and regeneration of functional tissues is a coveted goal of tissue repair.[40] On day 7, as visually revealed form the comparison of scar formation, the PGLA@CS treated wound displays a smooth and clear appearance without scar left when compared to the other groups.

Wound repairing, one of the most complex biological events, involves several processes including inflammation, cell proliferation, collagen regeneration and angiogenesis to restore tissue integrity and function.[41,42] So, in order to deeply understand the wound healing process, we performed histological analyses of wound tissue on day 4 after different treatments. In hematoxylin and eosin (H&E) staining images, detected are some basic epithelial structures and reconstruction of dermis tissue (Fig. 4a). In comparison, PGLA@CS-treated wound displayed much better healing effect than the other groups with respect to epithelial regeneration and incision closure. It can be observed that PGLA@CS-treated wound is already regenerated the integrated and continuous epidermis with the normal thickness, whereas the wounds in control groups (untreated wound, sPGLA, sPGLA+CS) present lowly repaired epidermis and epidermal hyperplasia, indicative of more chances of scar formation. Besides, fewer inflammation-related cells were found in sPGLA@CS-treated group, suggesting the strong anti-inflammatory response and the accelerated wound healing process due to CS coating. In addition, Masson's trichrome was used to stain collagen in tissue slice (Fig. 4b). Collagen Regeneration could facilitate new tissue growth during wound recovery. We found a larger blue-color area representing collagen below the epidermis in sPGLA@CS group. Semi-quantitative statistical analysis was conducted by Image J about collagen area (Fig. 4c). The collagen deposition increases from 18% in sPGLA group to 25% in sPGLA@CS group. In addition, the tissue slices were also analyzed by Image J. The incision length and depth in sPGLA@CS group are about 50% shorter in width and 83% less in depth compared to those in sPGLA group (Fig. S2 in ESI).

As mentioned above, H&E staining analysis manifested the infiltration of fewer inflammatory cell in wound sites slice due to CS coating on sutures, suggesting the stronger capability of CS-coated sutures for inflammation inhibition. To better understand this important effect, the expression levels of the classical inflammation-related cytokines around wounds were examined by ELISA assays on day 4 after different sutures treatments (Fig. 4d). IL (Interleukin)-10 is among the main inflammatory and immunosuppressive factors and participates in cellular growth regulation and differentiation. Under the regulation of IL-10, both innate and adaptive immune and inflammation response could be suppressed to protect the host from immune-meditated tissue damage, perturbed wound healing and scar formation.[43,44] The data show that the relative level of IL-10 (compared to the total protein in wound) in PGLA@CS group considerably increases whereas IL-10 in other groups remain almost unchanged. IL-6 and TNF-*α* are two proinflammatory cytokines and function as master regulator of inflammatory responses with fully pleotropic effects in various cell types. The expression levels of IL-6 and TNF-*α* would markedly rise in patients after surgery and acute infection.[45,46] It has been documented that myofibroblast differentiation has association with the upregulation of IL-6, which induces excessive fibrosis and promotes scar formation in surgical sites.[47] Resultant data show the in comparison with sPGLA treatment, there appears a profound decline of IL-6 and TNF-*α* expressed in sPGLA@CS group by 69.00% and 64.78%, respectively. Compared to untreated wound, sPGLA treatment seemed to induce even worse inflammation, which may relate with the tissue rejection to the implanted sutures. In contrast, sPGLA@CS indeed downregulated the expression of these pro-inflammatory mediators, reconfirming the positive contribution of CS coating. These results agreed

https://doi.org/10.1007/s10118-022-2770-9

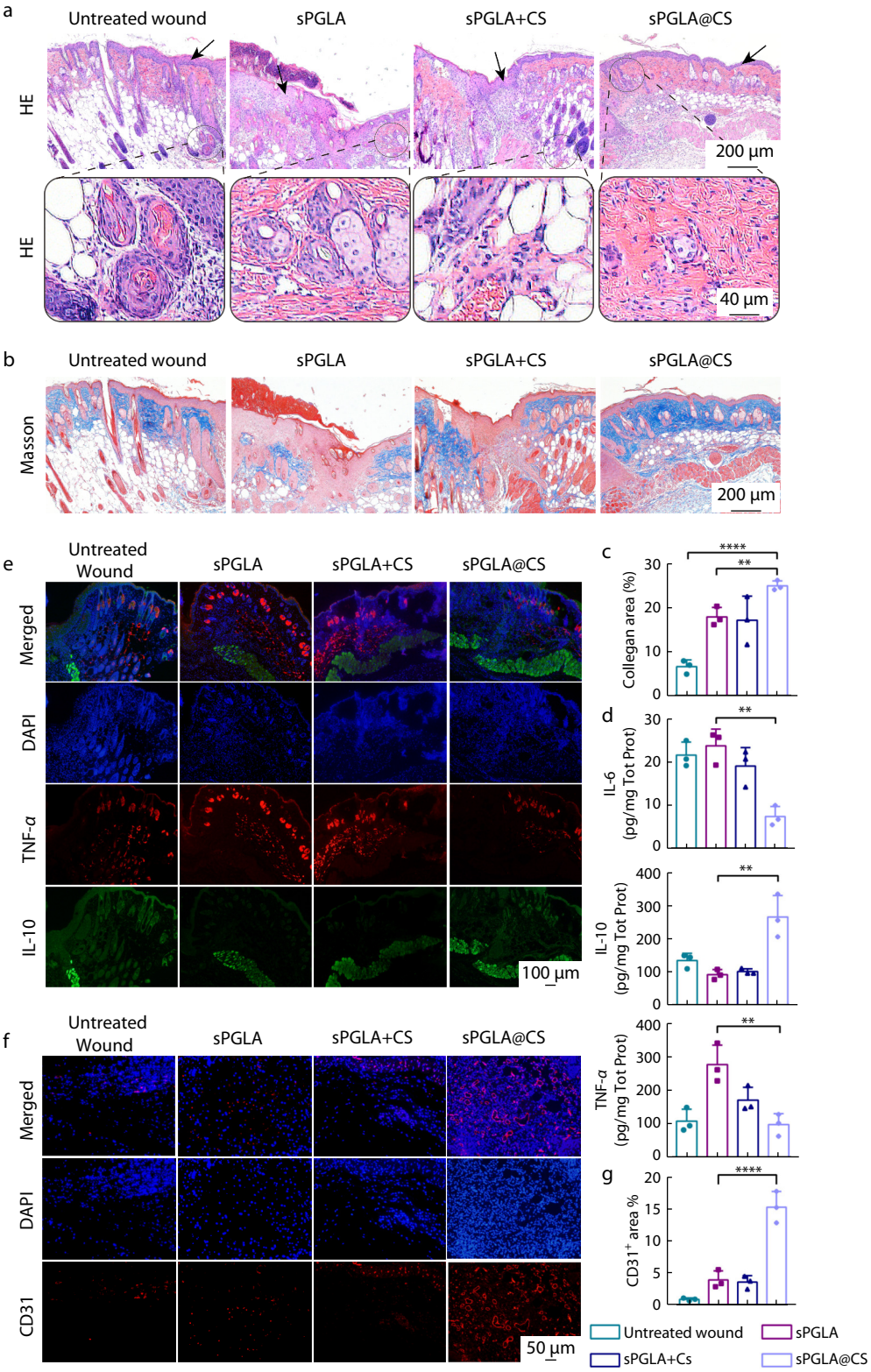


**Fig. 4** Variation of wound microenvironment after treatments with different sutures. (a) H&E staining images and (b) Masson's trichrome staining images of wounds treated with sutures on day 4. Black arrows indicated the rough interface between skin epidermis and dermis. Scale bar=200 μm. (c) Statistical data of collagen area in Masson's trichrome staining images analyzed by Image J. (d) ELISA data of IL-10, IL-6 and TNF-*α* expressed around wound sites after sutures treatments on day 4. (e) Immunofluorescence images of TNF-*α* (red), IL-10 (green) in wounds treated with sutures on day 4. Scale bar=100 μm. (f) Immunofluorescence images of $CD31^+$ cells (red) in wound sites on day 7 after suturing. Scale bar=50 μm. (g) Statistical data of $CD31^+$ area in fluorescence images analyzed by Image J. All data were shown as mean with SD. Statistical significance was calculated by one-way ANOVA. $^{**}p<0.01$, $^{***}p<0.001$, $^{****}p<0.0001$.

https://doi.org/10.1007/s10118-022-2770-9

well with the visual observation on IL-10$^+$/TNF-$\alpha^+$ cells in wound by immunofluorescence staining (Fig. 4e). The wounds in PGLA@CS group show significantly reduced intensity of TNF-$\alpha^+$ (red) signals together with the increased intensity of IL-10$^+$ (green) signals.

Inflammation relief and collagen regeneration would provide matrix to benefit tissue remodeling and thus neovascularization.[40,41] To investigate the influences of CS coating over neovascularization in wound sites, we measured the expression level of CD31, the vascular endothelial cell markers, by immunocytochemical staining (Fig. 4f). As expected, CD31$^+$ fluorescence occupied a larger proportion in the slice of PGLA@CS group compared to the controls, indicating angiogenesis and the remodeling in vascular network under sPGLA@CS treatment. Semi-quantitative statistical data show CD31$^+$ fluorescence in sPGLA@CS group increases by three times compared with that in sPGLA group (Fig. 4g). Overall, all the experimental results demonstrated that coating CS on sutures by our technique could relieve wound inflammation, stimulate collagen deposition, regenerate blood vessels, and assist tissue repairing, consequently leading to a significant enhancement of wound healing effect.

### *In vivo* Antibacterial Efficiency of Wounds Challenged by Bacteria

The favorable *in vitro* anti-bacterial performance and *in vivo* wound healing effect encouraged us to further investigate the defense of CS-coated sutures against *in vivo* acute bacterial infections. 20 mm Full-thickness longitudinal incision were made on each mouse back, and 50 μL of *E. coli* 25922 ($1\times10^8$ CFU/mL) was introduced onto the cutting wound to establish the model with *in situ* acute *E. coli* 25922 pathogen infection. After receiving suturing treatment, the postoperative wounds were immediately photographed (Fig. 5a). The infection and

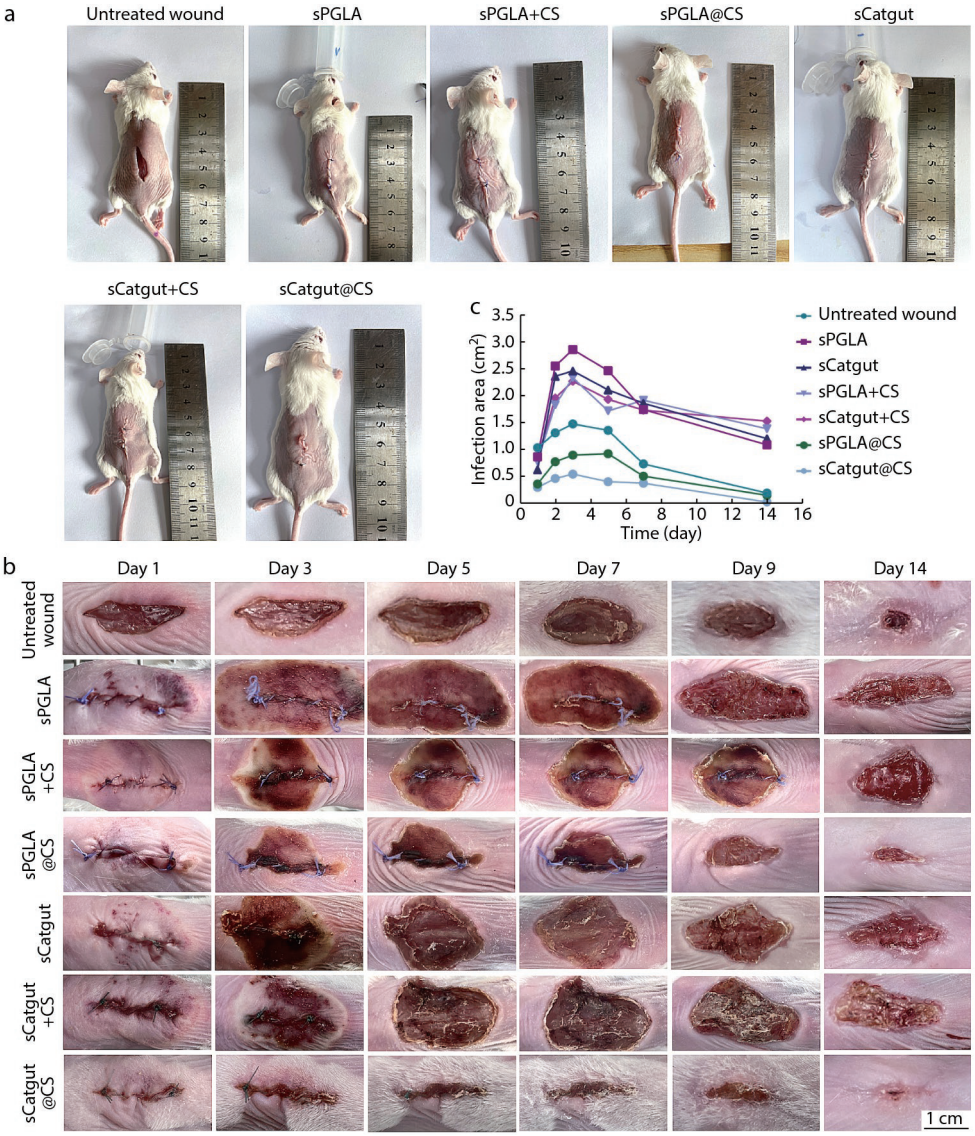


**Fig. 5** Acute infection resistance *in vivo*. (a) Pictures of the mice on day 0 after surgery. (b) Representative photos of the *E. coli* 25922 infected wound on day 1, 3, 5, 7, 9, and 14 after treatments by sPGLA, sCatgut, sPGLA+CS, sCatgut+CS, sPGLA@CS and sCatgut@CS. Scar bar=1cm. (c) Statistical data of infection area within 14 days provided by Image J.

https://doi.org/10.1007/s10118-022-2770-9

recovery in wound sites were recorded by photographs on day 1, 3, 5, 7, 9, and 14 (Fig. 5b). Visually, there are significant differences of infection degree among groups of untreated wounds, sPGLA, sCatgut, sPGLA+CS, sCatgut+CS, sPGLA@CS and sCatgut@CS. The untreated wound is in a bad status in surgical sites. Unfortunately, treatments with sPGLA, sCatgut, sPGLA+CS and sCatgut+CS offered even worse outcomes, including the widespread infection, serious tissue damages with ischemia and suppuration. It has been documented that the introduced sutures could increase the SSI risk. Sutures would closely contact with surgical site for a long time, which provide a "natural shelter" for bacterial adherence and colonization. This issue is more evident in braided absorbable sutures since the large amounts of gaps between strands of braided sutures provide a suitable environment for bacterial retention and biofilm formation, which largely increase the biological toxicity and infection area of SSI.I.[48–50] Our finding agreed well with the reported result that the sutures may aggravate infection. In comparison, treatments with sPGLA@CS and sCatgut@CS effectively inhibited the bacterial proliferation and accelerated wound healing. This conclusion was reconfirmed by the semi-quantitative analysis of the infection area in wound sites (Fig. 5c). The experimental results verified that CS-coated sutures provided excellent healing performance *in vivo* of the wounds challenged by pathogenic infection.

## CONCLUSIONS

Absorbable materials, particularly absorbable sutures are playing essential roles in surgical fields. Antibacterial activity is thought as one indispensable feature of the next generation of absorbable sutures. It seems that the existing approaches for the manufacture of antibacterial absorbable sutures are not suitable for the practical translation. We reported here a "gradient deposition" technique to coat a continuous and smooth layer of chitosan on the surface of absorbable sutures. *In vitro* and *in vivo* results demonstrated that coating CS on sutures by our technique could relieve wound inflammation, stimulate collagen deposition, regenerate blood vessels, and assist tissue repairing, consequently leading to significant enhancement of wound healing effect. This technique is highlighted with low cost, extreme convenience and excellent safety without organic solvents. Furthermore, the "gradient deposition" technique would not affect the fundamental properties of matrix and thus hold promises as a universal way for surfacial antibacterial modification toward almost all the surgical implanted materials, including but not limited to absorbable sutures.

## NOTES

The authors declare no competing financial interest.

### Electronic Supplementary Information

Electronic supplementary information (ESI) is available free of charge in the online version of this article at http://doi.org/10.1007/s10118-022-2770-9.

## ACKNOWLEDGMENTS

This work was financially supported by the National Natural Science Foundation of China (Nos. 51973164, 52131302, 22135005 and 51833007), National Key Research and Development Program of China (2019YFA0905603) and Fundamental Research Funds for the Central Universities (No. 2042021kf0037). All of the animal experiments were conducted under protocols approved by the Institutional Animal Care and Use Committee (IACUC) of the Animal Experiment Center of Wuhan University (Wuhan, P. R. China).

## REFERENCES

1 Dennis, C.; Sethu, S.; Nayak, S.; Mohan, L.; Morsi, Y.; Manivasagam, G. Suture materials—current and emerging trends. *J. Biomed. Mater. Res. A* **2016**, *104*, 1544–1559.
2 de la Harpe, K. M.; Kondiah, P. P. D.; Marimuthu, T.; Choonara, Y. E. Advances in carbohydrate-based polymers for the design of suture materials: a review. *Carbohydr. Polym.* **2021**, *261*, 117860.
3 Pillai, C. K. S.; Sharma, C. P. Review paper: absorbable polymeric surgical sutures: chemistry, production, properties, biodegradability, and performance. *J. Biomater. Appl.* **2010**, *25*, 291–366.
4 Ashraf, I.; Butt, E.; Veitch, D.; Wernham, A. Dermatological surgery: an update on suture materials and techniques. Part 1. *Clin. Exp. Dermatol.* **2021**, *46*, 1400–1410.
5 Abhari, R. E.; Martins, J. A.; Morris, H. L.; Mouthuy, P. A.; Carr, A. Synthetic sutures: clinical evaluation and future developments. *J. Biomater. Appl.* **2017**, *32*, 410–421.
6 Taylor, J. S.; Marten, C. A.; Potts, K. A.; Cloutier, L. M.; Cain, K. E.; Fenton, S. L.; Tatum, T. N.; James, D. A.; Myers, K. N.; Hubbs, C. A.; Burzawa, J. K.; Vachhani, S.; Nick, A. M.; Meyer, L. A.; Graviss, L. S.; Ware, K. M.; Park, A. K.; Aloia, T. A.; Bodurka, D. C.; Levenback, C. F.; Schmeler, K. M. What is the real rate of surgical site infection? *J. Oncol. Pract.* **2016**, *12*, e878–e883.
7 Wagner, J. C.; Wetz, A.; Wiegering, A.; Lock, J. F.; Löb, S.; Germer, C. T.; Klein, I. Successful surgical closure of infected abdominal wounds following preconditioning with negative pressure wound therapy. *Langenbeck. Arch. Surg.* **2021**, *406*, 2479–2487.
8 Renko, M.; Paalanne, N. Tapiainen, T.; Hinkkainen, M.; Pokka, T.; Kinnula, S.; Sinikumpu, J. J.; Uhari, M.; Serlo, W. Triclosan-containing sutures versus ordinary sutures for reducing surgical site infections in children: a double-blind, randomised controlled trial. *Lancet. Infect. Dis.* **2017**, *17*, 50–57.
9 Tummalapalli, M.; Anjum, S.; Kumari, S.; Gupta, B. Antimicrobial surgical sutures: recent developments and strategies. *Polym. Rev.* **2016**, *56*, 607–630.
10 Fields, A. C.; Pradarelli, J. C.; Itani, K. M. F. Preventing surgical site infections: looking beyond the current guidelines. *JAMA* **2020**, *323*, 1087–1088.
11 Wu, X.; Kubilay, N. Z.; Ren, J.; Allegranzi, B.; Bischoff, P.; Zayed, B.; Pittet, D.; Li, J. Antimicrobial-coated sutures to decrease surgical site infections: a systematic review and meta-analysis. *Eur. J. Clin. Microbiol.* **2017**, *36*, 19–32.
12 Deng, X.; Qasim, M.; Ali, A. Engineering and polymeric composition of drug-eluting suture: a review. *J. Biomed. Mater. Res. A* **2021**, *109*, 2065–2081.
13 Alshomer, F.; Madhavan, A.; Pathan, O.; Song, W. Bioactive sutures: a review of advances in surgical suture functionalisation. *Curr. Med. Chem.* **2017**, *24*, 215–223.
14 Lee, J.; Yoo, J.; Kim, J.; Jang, Y.; Shin, K.; Ha, E.; Ryu, S.; Kim, B. G.; Wooh, S.; Char, K. Development of multimodal antibacterial surfaces using porous amine-reactive films incorporating

lubricant and silver nanoparticles. *ACS Appl. Mater. Interfaces* **2019**, *11*, 6550–6560.
15 Wang, X.; Liu, P.; Wu, Q.; Zheng, Z.; Xie, M.; Chen, G.; Yu, J.; Wang, X.; Li, G.; Kaplan, D. Sustainable antibacterial and anti-inflammatory silk suture with surface modification of combined-therapy drugs for surgical site infection. *ACS Appl. Mater. Interfaces* **2022**, *14*, 11177–11191.
16 Serrano, C.; García-Fernández, L.; Fernández-Blázquez, J. P.; Barbeck, M.; Ghanaati, S.; Unger, R.; Kirkpatrick, J.; Arzt, E.; Funk, L.; Turón, P.; del Campo, A. Nanostructured medical sutures with antibacterial properties. *Biomaterials* **2015**, *52*, 291–300.
17 Benesch, J.; Tengvall, P. Blood protein adsorption onto chitosan. *Biomaterials* **2002**, *23*, 2561–2568.
18 Kim, U. J.; Lee, Y. R.; Kang, T. H.; Choi, J. W.; Kimura, S.; Wada, M. Protein adsorption of dialdehyde cellulose-crosslinked chitosan with high amino group contents. *Carbohydr. Polym.* **2017**, *163*, 34–42.
19 Shi, X. W.; Li, X. X.; Du, Y. M. Recent progress of chitin-based materials. *Acta Polymerica Sinica* (in Chinese) **2011**, 1–17.
20 Xia, G. X.; Wu, Y. M.; Bi, Y. F.; Chen, K.; Zhang, W. W.; Liu, S. Q.; Zhang, W. J.; Liu, R. H. Antimicrobial properties and application of polysaccharides and their derivatives. *Chinese J. Polym. Sci.* **2021**, *39*, 133–146.
21 Li, J.; Wu, Y.; Zhao, L. Antibacterial activity and mechanism of chitosan with ultra high molecular weight. *Carbohydr. Polym.* **2016**, *148*, 200–205.
22 Benchamas, G.; Huang, G.; Huang, S.; Huang, H. Preparation and biological activities of chitosan oligosaccharides. *Trends Food. Sci. Tech.* **2021**, *107*, 38–44.
23 Shariatinia, Z. Pharmaceutical applications of chitosan. *Adv. Colloid Interface Sci.* **2019**, *263*, 131–194.
24 Ghasemzadeh, H.; Sheikhahmadi, M.; Nasrollah, F. Full polysaccharide crosslinked-chitosan and silver nano composites, for use as an antibacterial membrane. *Chinese J. Polym. Sci.* **2016**, *34*, 949–964.
25 Avcu, E.; Baştan, F. E.; Abdullah, H. Z.; Rehman, M. A. U.; Avcu, Y. Y.; Boccaccini, A. R. Electrophoretic deposition of chitosan-based composite coatings for biomedical applications: a review. *Prog. Mater. Sci.* **2019**, *103*, 69–108.
26 Boon-in, S.; Theerasilp, M.; Crespy, D. Marrying the incompatible for better: Incorporation of hydrophobic payloads in superhydrophilic hydrogels. *J. Colloid Interface Sci.* **2022**, *622*, 75–86.
27 Abdelkader, A.; Fathi, H. A.; Hamad, M. A.; Elsabahy, M. Nanomedicine: a new paradigm to overcome drug incompatibilities. *J. Pharm. Pharmacol.* **2020**, *72*, 1289–1305.
28 Qin, B.; Fei, C.; Bridges Andrew, A.; Mashruwala Ameya, A.; Stone Howard, A.; Wingreen Ned, S.; Bassler Bonnie, L. Cell position fates and collective fountain flow in bacterial biofilms revealed by light-sheet microscopy. *Science* **2020**, *369*, 71–77.
29 Ciofu, O.; Moser, C.; Jensen, P. O.; Hoiby, N. Tolerance and resistance of microbial biofilms. *Nat. Rev. Microbiol.* **2022**, DOI: 10.1038/s41579-022-00682-4
30 Hall-Stoodley, L.; Costerton, J. W.; Stoodley, P. Bacterial biofilms: from the natural environment to infectious diseases. *Nat. Rev. Microbiol.* **2004**, *2*, 95–108.
31 Mahesh, L.; Kumar, V. R.; Jain, A.; Shukla, S.; Aragoneses, J. M.; Martínez González, J. M.; Fernández-Domínguez, M.; Calvo-Guirado, J. L. Bacterial adherence around sutures of different material at grafted site: a microbiological analysis. *Materials* **2019**, *12*, 2848.
32 Katz, S.; Izhar, M.; Mirelman, D. Bacterial adherence to surgical sutures: a possible factor in suture induced infection. *Ann. Surg.* **1981**, *194*, 35–41.
33 Ali-Mucheru, M. N.; Seville, M. T.; Miller, V.; Sampathkumar, P.; Etzioni, D. A. Postoperative surgical site infections: understanding the discordance between surveillance systems. *Ann. Surg.* **2020**, *271*, 94–99.
34 Wills, B. W.; Smith, W. R.; Arguello, A. M.; McGwin, G.; Ghanem, E. S.; Ponce, B. A. Association of surgical jacket and bouffant use with surgical site infection risk. *JAMA Surg.* **2020**, *155*, 323–328.
35 Alverdy, J. C.; Hyman, N.; Gilbert, J. Re-examining causes of surgical site infections following elective surgery in the era of asepsis. *Lancet. Infect. Dis.* **2020**, *20*, e38–e43.
36 Tomihata, K.; Suzuki, M.; Oka, T.; Ikada, Y. A new resorbable monofilament suture. *Polym. Degrad. Stab.* **1998**, *59*, 13–18.
37 Hu, W.; Huang, Z. M. Biocompatibility of braided poly(L-lactic acid) nanofiber wires applied as tissue sutures. *Polym. Int.* **2010**, *59*, 92–99.
38 Baygar, T.; Sarac, N.; Ugur, A.; Karaca, I. R. Antimicrobial characteristics and biocompatibility of the surgical sutures coated with biosynthesized silver nanoparticles. *Bioorg. Chem.* **2019**, *86*, 254–258.
39 Korntner, S.; Lehner, C.; Gehwolf, R.; Wagner, A.; Grütz, M.; Kunkel, N.; Tempfer, H.; Traweger, A. Limiting angiogenesis to modulate scar formation. *Adv. Drug Deliver. Rev.* **2019**, *146*, 170–189.
40 Konieczny, P.; Naik, S. Healing without scarring. *Science* **2021**, *372*, 346–347.
41 Willenborg, S.; Eming Sabine, A. Cellular networks in wound healing. *Science* **2018**, *362*, 891–892.
42 Rodrigues, M.; Kosaric, N.; Bonham, C. A.; Gurtner, G. C. Wound healing: a cellular perspective. *Physiol. Rev.* **2018**, *99*, 665–706.
43 Ip, W. K. E.; Hoshi, N.; Shouval Dror, S.; Snapper, S.; Medzhitov, R. Anti-inflammatory effect of IL-10 mediated by metabolic reprogramming of macrophages. *Science* **2017**, *356*, 513–519.
44 Sato, Y.; Ohshima, T.; Kondo, T. Regulatory role of endogenous Interleukin-10 in cutaneous inflammatory response of murine wound healing. *Biochem. Biophys. Res. Commun.* **1999**, *265*, 194–199.
45 Sun, W.; Wu, Y.; Zheng, M.; Yang, Y.; Liu, Y.; Wu, C.; Zhou, Y.; Zhang, Y.; Chen, L.; Li, H. Discovery of an orally active small-molecule tumor necrosis factor-*α* inhibitor. *J. Med. Chem.* **2020**, *63*, 8146–8156.
46 Yu, Q. J.; Fen, Z, C.; Huang, L. P.; He, J. W.; Zhou, Z. L.; Liu, F. Ellagic acid (EA), a tannin was isolated from *Eucalyptus citriodora* leaves and its anti-inflammatory activity. *Med. Chem. Res.* **2021**, *30*, 2277–2288.
47 Johnson, B. Z.; Stevenson, A. W.; Prêle, C. M.; Fear, M. W.; Wood, F. M. The role of IL-6 in skin fibrosis and cutaneous wound healing. *Biomedicines* **2020**, *8*, 101–119.
48 Leknes, K. N.; Selvig, K. A.; Boe, O. E.; Wikesjö, U. M. E. Tissue reactions to sutures in the presence and absence of anti-infective therapy. *J. Clin. Periodontol.* **2005**, *32*, 130–138.
49 Masini, B. D.; Stinner, D. J.; Waterman, S. M.; Wenke, J. C. Bacterial adherence to suture materials. *J. Surg. Educ.* **2011**, *68*, 101–104.
50 Markel, D. C.; Bergum, C.; Wu, B.; BouAkl, T.; Ren, W. Does suture type influence bacterial retention and biofilm formation after irrigation in a mouse model? *Clin. Orthop. Relat. Res.* **2019**, *477*, 116–126.

https://doi.org/10.1007/s10118-022-2770-9